PHYSICAL REVIEW A VOLUME 2, NUMBER 5 NOVEMBER 1970

Adiabatic Corrections in a Simple Model of Two Interacting Electronic-Potential Curves*

M. García Sucre
Departamento de Física Atómica y Molecular, Instituto Venezolano de Investigaciones Científicas, Apartado 1827, Caracas, Venezuela
and
F. Goychman and R. Lefebvre
Laboratoire de Photophysique Moléculaire,† *Faculté des Sciences, 91-Orsay, France*

(Received 9 June 1970)

Accurate numerical methods are applied to the vibronic problem resulting from two interacting intersecting harmonic curves. Two examples are considered, corresponding to either degenerate or nondegenerate electronic states. The energies are obtained with (a) the zeroth-order Born-Oppenheimer approximation; (b) the so-called adiabatic approximation, which includes the diagonal corrections to (a); (c) the full vibronic procedure. Several features in the correlation diagrams giving the energies as a function of the configuration-interaction matrix element are given an explanation. We also note that, in the model treated here, inclusion of the diagonal corrections does not always lead to an improvement of the energies.

I. INTRODUCTION

There are various circumstances where it is necessary to go beyond the usual Born-Oppenheimer (BO) approach for treating a system of electrons and nuclei. For molecules with degenerate or quasidegenerate electronic states, this may be essential, since the near equality of electronic and vibrational excitation energies may lead to a dynamic correlation between electrons and nuclei. Examples are the Jahn-Teller[1] or pseudo-Jahn-Teller[2] effect, the Renner effect,[3] the exciton-phonon coupling in dimers[4] and, more generally, in molecular aggregates.[5] For normal molecules, accurate calculations (say within cm^{-1}) are usually done by including the so-called diagonal corrections to the zeroth-order BO approximation.[6] This is based on the implicit assumption that this way of including the coupling between electrons and nuclei (sometimes called the adiabatic approximation) will produce better results than those of the zeroth-order treatment. However, the range of validity (if any) of this assumption is not clear (cf. for instance the recent review by Hirschfelder and Meath[7]).

Let us recall that for a system of electrons and nuclei the total wave function may be written[8]

$$\psi(q, Q)=\sum_m \phi_m(q, Q)\chi_m(Q) , \qquad (1)$$

where q and Q stand for the electronic and nuclear coordinates, respectively, and the $\phi_m(q, Q)$'s are the solutions of the electronic wave equation. The variational principle applied to Eq. (1) leads for the nuclear functions $\chi_m(Q)$ to the set of coupled equations

$$[T_N+E_m(Q)+C_{mm}(Q)-W]\chi_m(Q)+\sum_{n\neq m} C_{mn}(Q)\chi_n(Q)=0 , \qquad (2)$$

where T_N is the nuclear kinetic-energy operator, $E_m(Q)$ is the electronic energy associated with $\phi_m(q, Q)$, W is the total energy, and the $C_{mn}(Q)$'s are the quantities (for $m=n$) or operators (for $m\neq n$) which result from integration over electronic coordinates. The so-called adiabatic nuclear functions are the solutions of the decoupled equations

$$[T_N+E_m(Q)+C_{mn}(Q)]\chi_m^{\text{ad}}(Q)=W^{\text{ad}}\chi_m^{\text{ad}}(Q) , \qquad (3\text{a})$$

while the zeroth-order BO nuclear functions obey

$$[T_N+E_m(Q)]\chi_m^{\text{BO}}(Q)=W^{\text{BO}}\chi_m^{\text{BO}}(Q) . \qquad (3\text{b})$$

Going from (3b) to (3a) amounts to what is called introducing the diagonal corrections. The $C_{mn}(Q)$'s depend critically on the inverse of differences between electronic energies. Thus, when the diagonal corrections obtained by including the $C_{mn}(Q)$'s in the potential energies for the motion of nuclei are appreciable, there may be also significant nonadiabatic effects. A possible example of this situation is the first excited ${}^1\Sigma_g^+$ electronic state of the hydrogen molecule. Kolos and Wolniewicz have made a very careful study of this state.[9] Owing to configuration interaction between two electronic states with different equilibrium distances (Davidson[10]), the potential energy for this state shows two minima separated by a potential barrier of about 6000 cm^{-1}. The other electronic state resulting from the 2×2 configuration interaction is estimated to be about 6000 cm^{-1} above the top of the potential barrier. The diagonal corrections to the potential energy, due essentially to the nuclear kinetic-energy operator, are rather large for the lowest state (about 450 cm^{-1} near the critical internuclear distance corresponding to the smallest electronic splitting). Thus, for levels which are not located at the bottom of the wells, both adiabatic and nonadiabatic effects should be important. For such levels, Kolos and Wolniewicz have found that the zeroth-order energies are in fact better than the adiabatic ones.

The only theorem[11] at our disposal to relate the energies deduced from the various approaches concerns the ground state of a system of nuclei and electrons: The zeroth-order BO energy is a lower bound and the adiabatic energy an upper bound to the exact ground-state energy. This is obviously not sufficient to investigate the question raised above. In order to get some more insight into this problem, we have applied accurate numerical methods to a simple model.

II. MODEL

We consider two electronic states ϕ_1 and ϕ_2 depending on a single internal nuclear coordinate Q. The two electronic energies are harmonic, of force constant k, with their minima at $Q=\pm\lambda$, respectively; the separation between the equilibrium energies is noted as $2V$ (Fig. 1). Configuration interaction is assumed to mix the two states. The electronic problem is summarized by the set of matrix elements:

$$\langle\phi_1(q,Q)|H_{\mathrm{el}}|\phi_1(q,Q)\rangle_q=\tfrac{1}{2}k(Q-\lambda)^2+2V, \tag{4a}$$

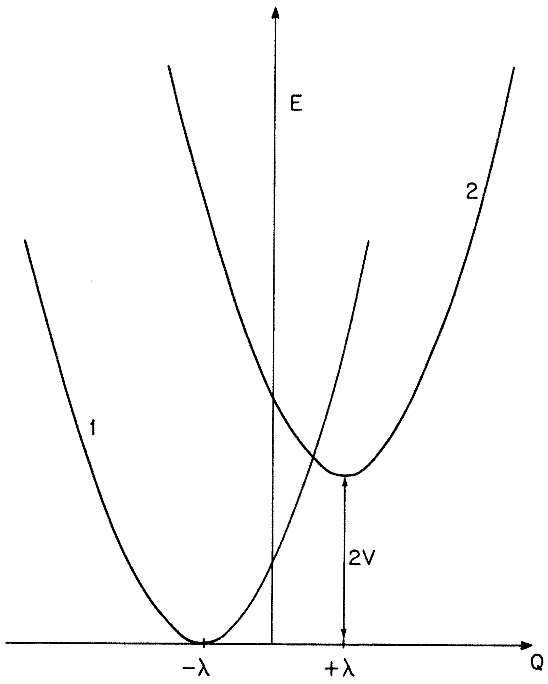

FIG. 1. Two harmonic electronic potential curves, of same force constant, with minima centered at $Q=-\lambda$ and $Q=+\lambda$, respectively, and with a vertical displacement $2V$.

$$\langle\phi_2(q,Q)|H_{\mathrm{el}}|\phi_2(q,Q)\rangle_q=\tfrac{1}{2}k(Q+\lambda)^2, \tag{4b}$$

$$\langle\phi_1(q,Q)|H_{\mathrm{el}}|\phi_2(q,Q)\rangle_q=\langle\phi_2(q,Q)|H_{\mathrm{el}}|\phi_1(q,Q)\rangle_q=v, \tag{4c}$$

where the subscript q means integration only over electronic coordinates. The mixing produces the two states

$$\phi^{\pm}(q,Q)=c_1^{\pm}(Q)\,\phi_1(q,Q)+c_2^{\pm}(Q)\phi_2(q,Q), \tag{5}$$

with coefficients

$$\begin{aligned} c_1^{-}(Q)&=(v/\sqrt{2})\{v^2+(kQ\lambda-V)^2\\ &\qquad\pm(kQ\lambda-V)[(kQ\lambda-V)^2+v^2]\}^{1/2},\\ c_2^{-}(Q)&=-(v/\sqrt{2})\{v^2+(kQ\lambda-V)^2\\ &\qquad\mp(kQ\lambda-V)[(kQ\lambda-V)^2+v^2]\}^{1/2},\\ c_1^{+}(Q)&=-c_2^{-}(Q),\quad c_2^{+}(Q)=c_1^{-}(Q)\,. \end{aligned} \tag{6}$$

The corresponding energies are

$$E^{\pm}(Q)=\tfrac{1}{2}k\lambda^2+V+\tfrac{1}{2}kQ^2\pm[(kQ\lambda-V)^2+v^2]^{1/2}.$$

If we assume that v is a constant: For $V=0$, $E^-(Q)$ is either a single-well or double-well potential for $v<k\lambda^2$ or $v>k\lambda^2$, while $E^+(Q)$ is always a single-well potential.

The vibronic wave function (the exact function within the model) can be written

$$\psi(q,Q)=\phi^+(q,Q)\chi^+(Q)+\phi^-(q,Q)\chi^-(Q). \tag{7}$$

We assume further that

$$T_N\phi_1=\phi_1T_N\,,\quad T_N\phi_2=\phi_2T_N\,. \tag{8}$$

Assumption (8) means that we would not expect the BO approximation to break down if we had only one of the electronic states. The consequence is that the adiabaticity of the electronic functions (5) resides in the mixing coefficients which for small values of v may vary rapidly with Q in the crossing region. T_N is the nuclear kinetic operator corresponding to the internal coordinate Q,

$$T_N=-\frac{\hbar^2}{2M}\frac{\partial^2}{\partial Q^2}\,. \tag{9}$$

We may mention at this point that the model is defined not in order to make the problem tractable (the methods used below to obtain the energies could be applied to arbitrary potential curves with a Q-dependent configuration-interaction matrix element) but to obtain the simplest case displaying the essential features of the coupled equations (10). With these assumptions, the two nuclear factors $\chi^+(Q)$ and $\chi^-(Q)$ obey the two equations

$$\begin{aligned}&[T_N+E^+(Q)+c_1^+(T_Nc_1^+)+c_2^+(T_Nc_2^+)-W]\chi^+(Q)+\Big[c_1^+(T_Nc_1^-)\\ &\quad+c_2^+(T_Nc_2^-)-\frac{\hbar^2}{M}\left(c_1^+\frac{\partial c_1^-}{\partial Q}+c_2^+\frac{\partial c_2^-}{\partial Q}\right)\frac{\partial}{\partial Q}\Big]\chi^-(Q)=0\end{aligned} \tag{10a}$$

and

$$\left[c_1^-(T_N c_1^+) + c_2^-(T_N c_2^+) - \frac{\hbar^2}{M}\left(c_1^- \frac{\partial c_1^+}{\partial Q} + c_2^- \frac{\partial c_2^+}{\partial Q}\right)\frac{\partial}{\partial Q}\right]\chi^+(Q)$$

$$+ [T_N + E^-(Q) + c_1^-(T_N c_1^-) + c_2^-(T_N c_2^-) - W]\chi^-(Q) = 0\,. \quad \text{(10b)}$$

The limited-configuration-interaction calculation leading to (5) is equivalent to replacing the electronic Schrödinger equation by a matrix equation

$$H \cdot \vec{c} = E\vec{c}\,, \qquad (11)$$

H being the matrix of elements given by (4). The two solutions are column vectors $\vec{C}^+$ and $\vec{C}^-$ obeying

$$H \cdot \vec{c}^- = E^-\vec{c}^-; \quad H \cdot \vec{c}^+ = E^+\vec{c}^+. \qquad (12)$$

We have the following set of identities:

$$\vec{c}^{-\dagger} \cdot \vec{c}^+ \frac{\partial E^+}{\partial Q} + E^+\vec{c}^{-\dagger} \cdot \frac{\partial \vec{c}^+}{\partial Q} = \vec{c}^{-\dagger} \cdot \frac{\partial}{\partial Q} E^+\vec{c}^+$$

$$= \vec{c}^{-\dagger} \cdot \frac{\partial}{\partial Q} H \cdot \vec{c}^+ = \vec{c}^{-\dagger} \cdot H \cdot \frac{\partial}{\partial Q}\vec{c}^+ + \vec{c}^{-\dagger} \cdot \frac{\partial H}{\partial Q} \cdot \vec{c}^+$$

$$= E^-\vec{c}^{-\dagger} \cdot \frac{\partial}{\partial Q}\vec{c}^+ + \vec{c}^{-\dagger} \cdot \frac{\partial H}{\partial Q}\vec{c}^+. \qquad (13)$$

Equation (13) can be rearranged as

$$\vec{c}^{-\dagger} \cdot \frac{\partial}{\partial Q}\vec{c}^+ = [E^+(Q) - E^-(Q)]^{-1}\vec{c}^{-\dagger} \cdot \frac{\partial H}{\partial Q} \cdot \vec{c}^+. \qquad (14)$$

This is very similar to the relation obtained with the exact solutions of the electronic wave equation[12]:

$$\left\langle \phi_m \middle| \frac{\partial}{\partial Q} \middle| \phi_n \right\rangle_q = [E_n(Q) - E_m(Q)]^{-1} \left\langle \phi_m \middle| \frac{\partial H_{\mathrm{el}}}{\partial Q} \middle| \phi_n \right\rangle_q .$$

In particular, (14) shows that the derivative of the electronic function (a vector in our case) with respect to a nuclear coordinate becomes large when the electronic splitting is small for some value of Q. Since this occurs at the crossing point Q_c when v is small,

$$E^+(Q_c) - E^-(Q_c) = 2v\,. \qquad (15)$$

We may also write

$$\frac{\partial}{\partial Q}\vec{c}^+ = \vec{c}^+\left(\vec{c}^{+\dagger} \cdot \frac{\partial}{\partial Q}\vec{c}^+\right) + \vec{c}^-\left(\vec{c}^{-\dagger} \cdot \frac{\partial}{\partial Q}\vec{c}^+\right)$$

$$= \vec{c}^-\left(\vec{c}^{-\dagger} \cdot \frac{\partial}{\partial Q}\vec{c}^+\right), \qquad (16)$$

$$\frac{\partial}{\partial Q}\vec{c}^- = \vec{c}^+\left(\vec{c}^{+\dagger} \cdot \frac{\partial}{\partial Q}\vec{c}^-\right) + \vec{c}^-\left(\vec{c}^{-\dagger} \circ \frac{\partial}{\partial Q}\vec{c}^-\right)$$

$$= \vec{c}^+\left(\vec{c}^{+\dagger} \cdot \frac{\partial}{\partial Q}\vec{c}^-\right), \qquad (17)$$

the simplification occurring because of the normalization of the vectors $\vec{c}^\pm$. Using (16) and (17) we obtain, for instance,

$$c_1^+ \frac{\partial^2 c_1^+}{\partial Q^2} + c_2^+ \frac{\partial^2 c_2^+}{\partial Q^2} = \vec{c}^{+\dagger} \cdot \frac{\partial^2}{\partial Q^2}\vec{c}^+$$

$$= \left(\vec{c}^{+\dagger} \cdot \frac{\partial}{\partial Q}\vec{c}^-\right)\left(\vec{c}^{-\dagger} \circ \frac{\partial}{\partial Q}\vec{c}^+\right), \qquad (18)$$

$$c_1^+ \frac{\partial^2 c_1^-}{\partial Q^2} + c_2^- \frac{\partial^2 c_2^-}{\partial Q^2} = \vec{c}^{+\dagger} \cdot \frac{\partial^2}{\partial Q^2}\vec{c}^- = \frac{\partial}{\partial Q}\left(\vec{c}^{+\dagger} \cdot \frac{\partial \vec{c}^-}{\partial Q}\right). \qquad (19)$$

Equations (18) and (19) are the counterpart in our problem of the general relation for the exact electronic wave functions[12]

$$\left\langle \phi_m \middle| \frac{\partial^2}{\partial Q^2} \middle| \phi_n \right\rangle = \sum_K \left\langle \phi_m \middle| \frac{\partial}{\partial Q} \middle| \phi_K \right\rangle \left\langle \phi_K \middle| \frac{\partial}{\partial Q} \middle| \phi_n \right\rangle$$

$$+ \frac{\partial}{\partial Q}\left\langle \phi_m \middle| \frac{\partial}{\partial Q} \middle| \phi_n \right\rangle. \qquad (20)$$

With the set of relations (14), (18), and (19), the diagonal corrections and coupling operators of Eq. (10) are easily obtained from the expressions (6) for the mixing coefficients.

III. CALCULATIONS

We now present and comment on some calculations performed with the above model. In order to make these calculations, we first of all introduce the dimensionless parameters

$$\alpha = 2^{-1/2}k\lambda^2/h\nu; \quad \beta = v/h\nu;$$

$$R = Q/\lambda \quad \text{with } h\nu = \hbar\left(\frac{k}{m}\right)^{1/2}.$$

The equations for the adiabatic vibrational functions $\chi^{\pm\mathrm{ad}}(R)$ take the form

$$\left(-\frac{\partial^2}{\partial R^2} + \frac{\alpha^2\beta^2}{[(V - 2\alpha R)^2 + \beta^2]^2} + 4\alpha(V + \alpha R^2)\right.$$

$$\left.\pm 4\alpha[(V - 2\alpha R)^2 + \beta^2]^{1/2} - W\right)\chi^{\pm\mathrm{ad}}(R) = 0\,.$$

The ± signs refer to the upper or lower potential curves. The BO and adiabatic results are obtained from a numerical integration of the Schrödinger equation with the Cooley-Cashion program.[13] The nonadiabatic (or vibronic) energies are obtained from a diagonalization procedure in a set of basis functions associated with the electronic curves before decrossing.

We have studied the two following cases: (a) degenerate situation ($V = 0$) for $\alpha = 1$ and a varying β (the energies are given in Fig. 2); (b) nondegenerate situation ($2V = 5h\nu$) for $\alpha = 1$ and a varying β (the energies are given in Fig. 3).

On these two correlation diagrams the descending curves give the energies associated with the lower potential and the ascending curves, those of the up-

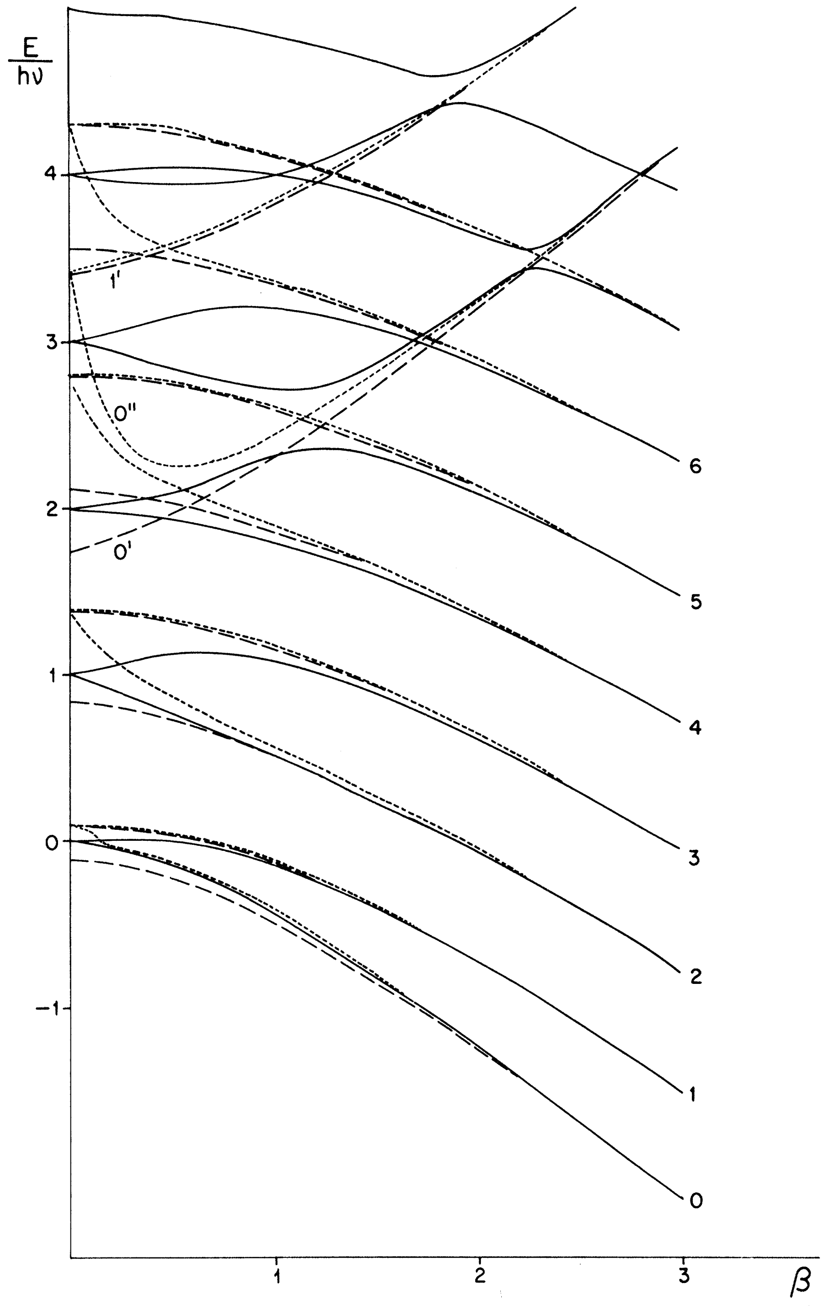

FIG. 2. Correlation diagrams for the zeroth-order BO (dashed curve), adiabatic (dotted curve), and exact vibronic (solid curve) energies, when $\alpha = 1$ for the degenerate case ($V=0$).

per potential. The full curves give the nonadiabatic energies.

In both cases, adiabatic and nonadiabatic effects vanish in the limit of a large coupling between electronic functions. Thus, for large β all three approaches lead to the same results. Table I gives the six lowest energies for $\beta = 1$ in the degenerate and nondegenerate cases. One may note the following: (i) The adiabatic energies do not always lie between the corresponding BO and vibronic levels. However, for the ground state we have $E_{\mathrm{BO}} < E_{\mathrm{vib}} < E_{\mathrm{ad}}$, in accordance with Brattsev's theorem. (ii) This order does not persist as we go to upper levels but adiabatic energies remain above the corresponding BO energies. This may be proved with the help of the Hellman-Feynman theorem. Let H^{ad} be the Hamiltonian of the adiabatic approximation, which can be written

$$H^{\mathrm{ad}} = H^{\mathrm{BO}} + \lambda A, \quad A = \vec{\mathrm{C}}^{\pm} \cdot T_N \vec{\mathrm{C}}^{\pm}, \quad \lambda = 1 .$$

A being positive everywhere, $\langle A \rangle$ is positive also. Since this is $\partial E(\lambda)/\partial\lambda$, this latter quantity is an increasing function of λ. Therefore, for all states $E^{n}_{\mathrm{BO}} < E^{n}_{\mathrm{ad}}$. (iii) As we go up in energy in case b

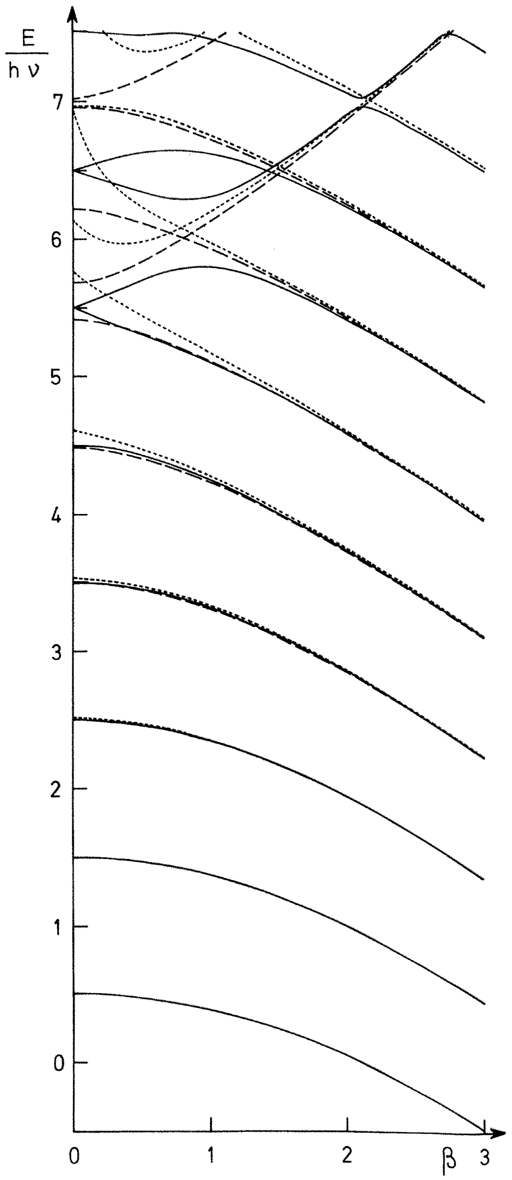

FIG. 3. Correlation diagrams for the zeroth-order BO (dashed curve), adiabatic (dotted curve), and exact vibronic (solid curve) energies when $\alpha = 1$ for a nondegenerated state ($2V = 5h\nu$).

TABLE I. Energies at $\beta = 1$ for the six lowest states in the degenerate case a, and the nondegenerate case b. The origin corresponds to the zero-point energy of the vibronic problem at zero coupling.

v	Case a			Case b		
	E^-_{BO}	E^-_{ad}	E_{vib}	E^-_{BO}	E^-_{ad}	E_{vib}
0	−1.2789	−1.2398	−1.2436	0.3834	0.3845	0.3842
1	−0.7375	−0.7182	−0.7316	1.3680	1.3712	1.3699
2	−0.0762	−0.0569	−0.0762	2.3444	2.3535	2.3349
3	0.6256	0.6410	0.6144	3.3047	3.3271	3.3151
4	1.3595	1.3737	1.3418	4.2738	4.2782	4.2495
5	2.1154	2.1282	2.0887	5.1094	5.1711	5.0965

(Table I), the BO energies become better than the adiabatic energies. This is reminiscent of the situation for the first ${}^1\Sigma_g^+$ excited state of H_2.[9]
(iv) A general rule concerns the adiabatic levels belonging to the lower potential and which are below a threshold corresponding to the lowest adiabatic level of the upper potential: These levels are always above the corresponding vibronic levels. This can be demonstrated by noting that the vibronic problem can be formulated as a configuration interaction calculation based on the adiabatic functions, with off-diagonal elements only between the functions belonging to the two different electronic states. Therefore, all levels below the threshold are necessarily pushed down.

IV. DETAILED DISCUSSION OF THE DEGENERATE CASE

The correlation diagrams for the degenerate case present several special features which, although probably of little practical interest, will now be commented on and explained. The two interacting potential curves are exchanged by the operating $Q \rightarrow -Q$. This results in the vibronic levels at zero coupling being degenerate by pairs. The adiabatic levels are also degenerate by pairs and this is a little less evident. Figure 4 shows the shape of the diagonal correction (the same in both electronic states) for $\alpha = 1$ and various values of β. When β is small, the correction is a sharp peak at $Q = 0$. This wall separates the two half-potentials for $Q > 0$ or $Q < 0$. The adiabatic vibrational functions which are anyway either even or odd under the operation $Q \rightarrow -Q$ become at the limit of zero coupling the even and odd combinations of the vibrational functions belonging to the half-potentials. These functions do not overlap because of the presence of the infinitely high barrier and therefore the two combinations have the same energy. This behavior was checked very carefully numerically. We may mention here that we disagree with Bierman who, in a similar problem concerning the vibronic levels of a dimer, has stated that the adiabatic energies go to the correct energies for a vanishingly small coupling.[14] Both kinds of levels show a twofold degeneracy at zero coupling, but are definitely different.

Another remarkable fact in Fig. 2 is the degeneracy of the odd BO levels with the adiabatic levels at $\beta = 0$. This is due to the fact that the vanishing of these BO functions at $Q = 0$ lead to a problem with the boundary conditions which govern also the adiabatic calculations.

The adiabatic corrections for different couplings and different vibrationals quantum numbers are given in Fig. 5 (odd levels) and Fig. 6 (even levels).

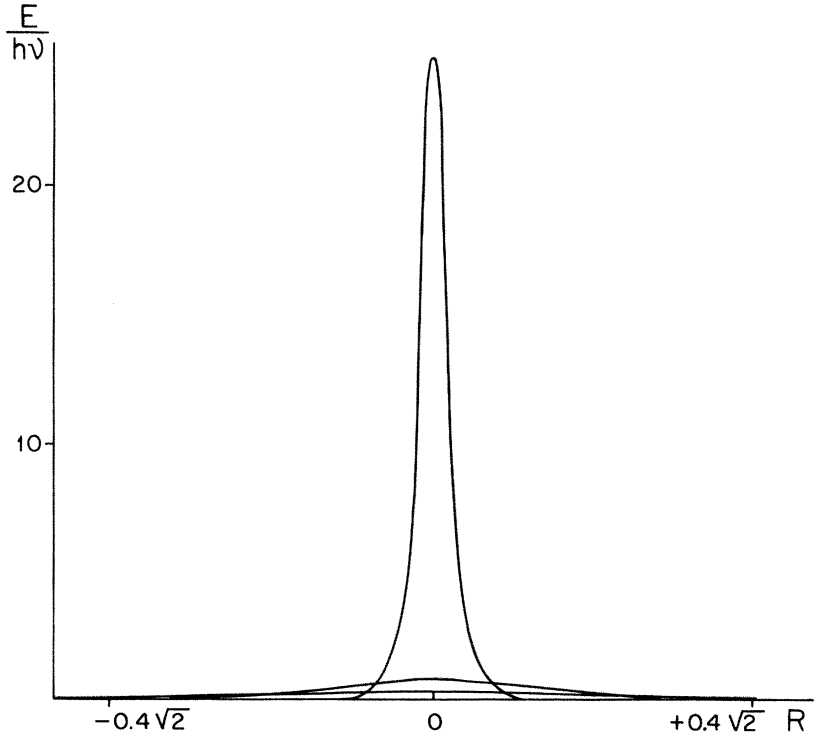

FIG. 4. Diagonal corrections $\vec{C}^{\pm\dagger}\cdot T_N\vec{C}^{\pm}$ for $\alpha=1$ and different values of β. The sharp and narrow curve corresponds to $\beta=0.1$; the other curves correspond in decreasing order to $\beta=0.6$ and $\beta=1.1$, respectively.

We give now a succinct explanation for the various regularities which are observed in these two diagrams.

The corrections for odd levels are systematically smaller than those for the even levels. This is related to the vanishing of the odd wave functions in the region of the potential barrier. For β large enough, an increase in quantum number v decreases the correction, since this reduces the amplitude of the wave function. For small β there is a reverse effect which has a different origin for odd and even levels. For odd levels, the correction depends on

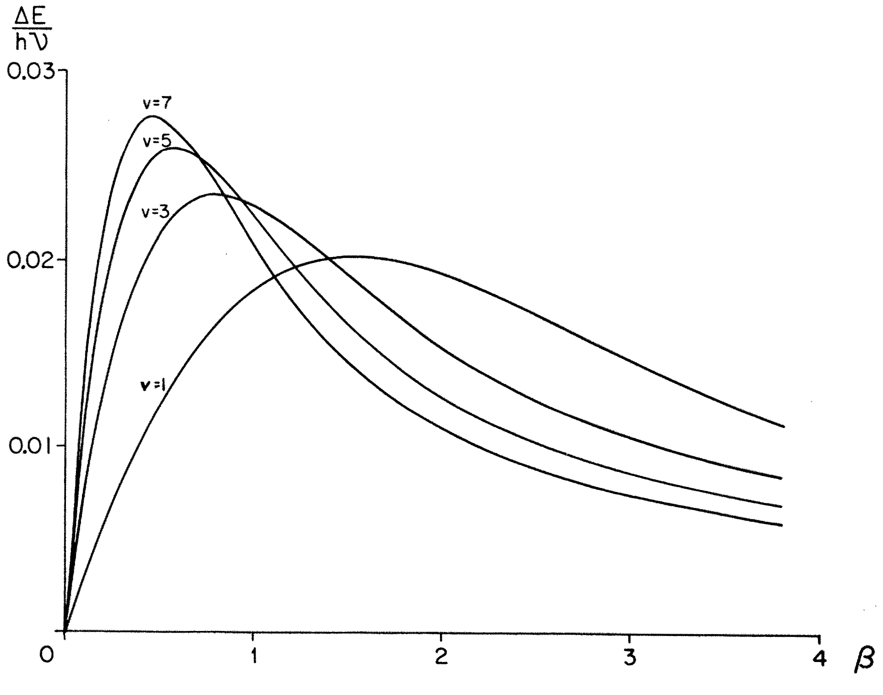

FIG. 5. Adiabatic corrections ΔE (in $h\nu$ units) for some odd levels ($v=1$, 3, 5, 7) of the lower potential, as a function of β, with $\alpha=1$.

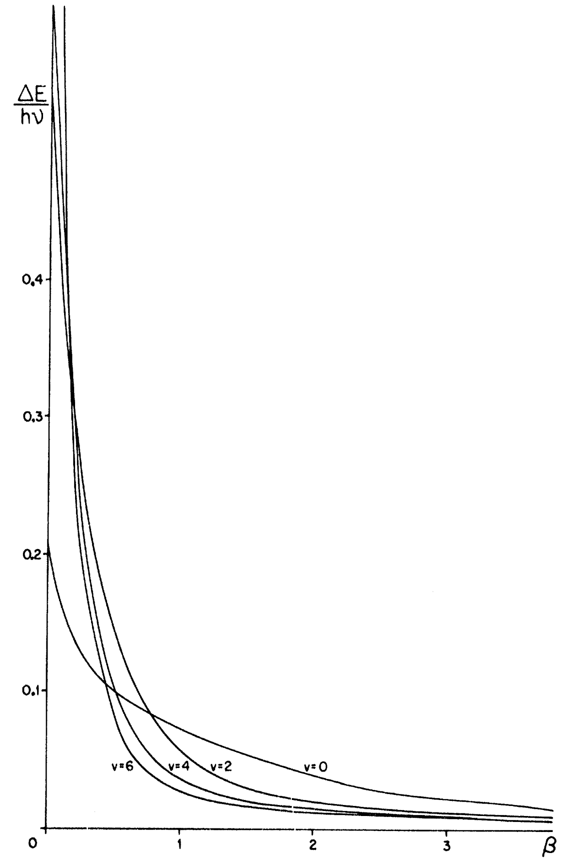

FIG. 6. Adiabatic corrections ΔE (in $h\nu$ units) for some even levels ($v=0$, 2, 4, 6) of the lower potential, as a function of β, with $\alpha=1$.

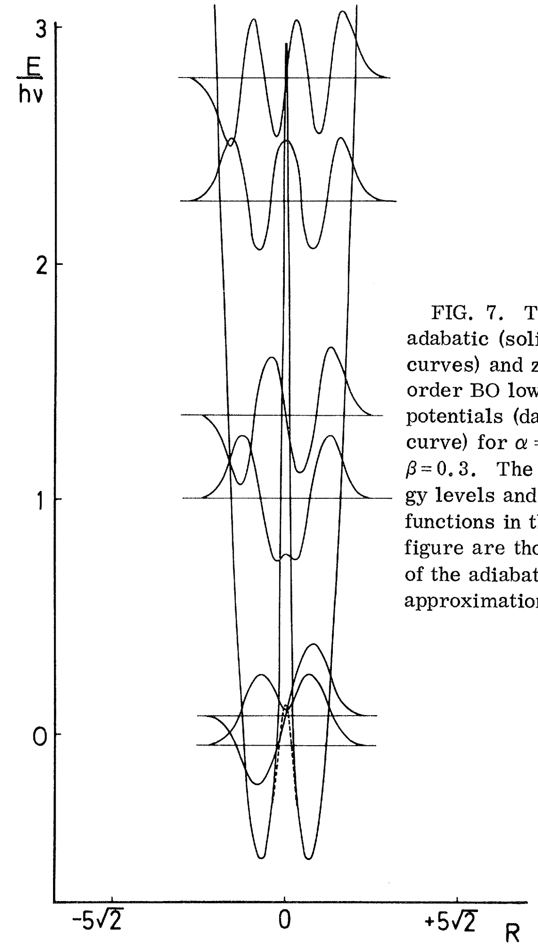

FIG. 7. The adabatic (solid curves) and zeroth-order BO lower potentials (dashed curve) for $\alpha=1$ and $\beta=0.3$. The energy levels and wave functions in the figure are those of the adiabatic approximation.

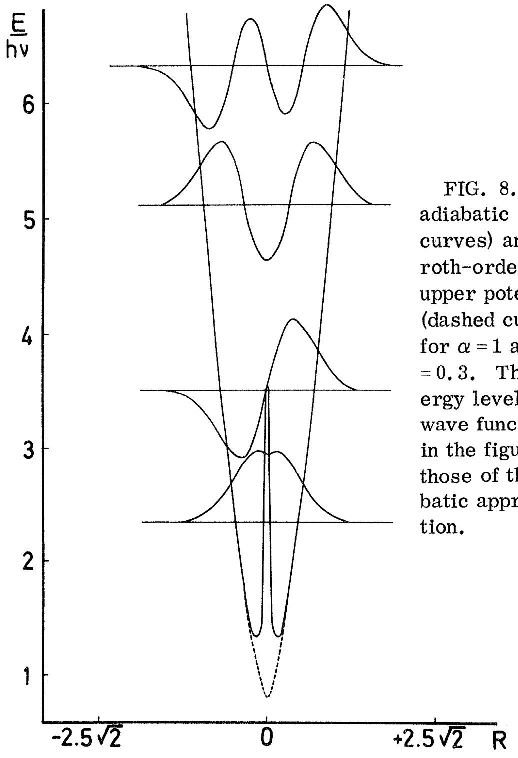

FIG. 8. The adiabatic (solid curves) and zeroth-order BO upper potentials (dashed curve) for $\alpha=1$ and $\beta=0.3$. The energy levels and wave functions in the figure are those of the adiabatic approximation.

the slope of the wave function in the region of the (now) narrow barrier, and this slope increases as the quantum number v increases. For even levels, the barrier produces a dip in the wave function which is more pronounced the smaller the vibrational quantum number.

Finally, Figs. 7 and 8 reproduce some of the adiabatic vibrational functions associated with the lower and upper potentials for $\beta=0.3$. Because of the diagonal contribution, both potentials present two wells. The two lowest even wave functions of the lower potential and the lowest even function of the upper potential already show the dip, which when the barrier gets higher and narrower will be present in all even functions.

V. CONCLUSIONS

Although based on a model, we think that the present treatment has enough of the essential features of a more realistic molecular calculation to indicate that the so-called adiabatic corrections are misnamed, since it may happen that the simple BO results are better than the adiabatic ones.

*A preliminary report was presented at the ASOVAC Meeting, Caracas, May, 1969 [Acta Cient. Venezolana, 20, 106 (1969)].

†Groupe de Recherches du CNRS, associé a la Faculté des Sciences d'Orsay.

[1] H. A. Jahn and E. Teller, Proc. Roy. Soc. (London) A161, 220 (1934).

[2] W. Moffit and A. D. Liehr, Phys. Rev. 106, 1195 (1957).

[3] E. Renner, Z. Physik 92, 172 (1934); J. A. Pople and H. C. Longuet-Higgins, Mol. Phys. 1, 372 (1958).

[4] A. Witkowski and W. Moffit, J. Chem. Phys. 33, 872 (1960).

[5] W. Siebrand, J. Chem. Phys. 40, 2231 (1964).

[6] W. Kolos and L. Wolniewicz, J. Chem. Phys. 41, 3663 (1964); 43, 2429 (1965); L. Wolniewicz, *ibid.* 45, 515 (1965).

[7] J. O. Hirschfelder and W. J. Meath, Advan. Chem. Phys. 12, 3 (1967).

[8] M. Born and J. R. Oppenheimer, Ann. Physik 84, 457 (1927); M. Born, Nachr. Ges. Wiss, Göttingen Math. Phys. Kl, 1 (1951).

[9] W. Kolos and L. Wolniewicz, J. Chem. Phys. 50, 3228 (1969).

[10] E. R. Davidson, J. Chem. Phys. 33, 1577 (1960).

[11] V. F. Brattsev, Dokl. Akad. Nauk SSSR 160, 570 (1965) [Soviet Phys. Doklady 10, 44 (1965)].

[12] W. Hobey and A. D. McLachlan, J. Chem. Phys. 33, 1695 (1960).

[13] J. W. Cooley, Math. Comp. XV, 363 (1961); J. K. Cashion, J. Chem. Phys. 39, 1872 (1963).

[14] A. Bierman, J. Chem. Phys. 45, 647 (1966).

PHYSICAL REVIEW A VOLUME 2, NUMBER 5 NOVEMBER 1970

Temperature Dependence of Hyperfine Pressure Shifts. II. Nitrogen in Helium, Neon, and Molecular Nitrogen†*

R. E. Weiss,‡ R. H. Lambert, and L. C. Balling
Department of Physics, University of New Hampshire, Durham, New Hampshire 03824

(Received 11 May 1970)

Spin-exchange optical pumping has been used to measure the hyperfine pressure shift of atomic nitrogen in helium, neon, and molecular nitrogen as a function of temperature. In the range 70–500 °C, the change in pressure shift was linear with temperature, and the values were for helium, $-(0.1\pm 0.1)\times 10^{-4}$; for neon, $(0.6\pm 0.1)\times 10^{-4}$; and for molecular nitrogen, $(1.4\pm 0.3)\times 10^{-4}$ in units of Hz/Torr °C. The measurements also give $A = 10\,450\,929.4 \pm 1.8$ Hz for the free atom. The quadrupole interaction constant was also measured and found to be independent of temperature and pressure. The value was $B = 1.3\pm 0.5$ Hz.

When the hyperfine structure of an atom is measured in the presence of a buffer gas, small frequency shifts are detected which depend essentially linearly[1] on the buffer-gas pressure. Theoretical attempts to understand these shifts indicate an expected dependence on the temperature of the buffer gas as well as on the density. With the recently discovered ability to optically pump over an extended temperature range,[2] it is now possible to investigate this aspect of the theory.

Recently we reported measurements of the temperature dependence of the hyperfine pressure shift of deuterium in helium.[3] The present paper describes similar measurements made on atomic nitrogen in helium, neon, and molecular nitrogen. Pressure shifts of atomic hydrogen (the isotopic mass dependence of these shifts is negligible[4]) and atomic nitrogen are of particular interest because of the recent extensive theoretical calculations made for them.[5,6]

The experiment consisted of the measurement of the hyperfine intervals of N^{14} at a variety of buffer-gas pressures and temperatures. By extrapolating to zero pressure, at fixed temperature, one is able to infer the free-atom magnetic dipole (A) and electric quadrupole (B) interaction constants. Although nitrogen would not be expected to have any ground-state hyperfine structure to first order if LS coupling were rigorously applicable,[7] Heald and Beringer[8] measured A to be 10.45 ± 0.02 MHz. Numerous measurements since then have confirmed and extended this value.[9–14]

The most recent theoretical[15] attempt to understand the dipole constant A, utilizing a many-body technique, predicts 10.49 ± 0.15 MHz. Core polarization accounts for 5.7 MHz of this, and correlation effects the remaining 4.8 MHz. The reported measurements using the maser[14] also reported a value of 1.3 ± 0.3 Hz for the quadrupole interaction constant B. Prior to this measurement, Holloway, Luscher, and Novick[12] attempted to predict B. Their calculation utilized only the ^2P and the ^2D levels in addition to the ^4S ground state which can be constructed from the $(1s)^2\,(2s)^2\,(2p)^3$ configuration. These levels are used in second-order perturbation theory with the magnetic dipole perturbation to get